12WCEE 2000

0278

LIQUEFACTION AND PARTICLE CRUSHING OF SOIL

Masayuki HYODO[1], Yukio NAKATA[2], Noritaka ARAMAKI[3], Adrian F L HYDE[4] And Shogo INOUE[5]

SUMMARY

The present study was performed in order to understand the effect of soil compressibility and crushability on the monotonic and cyclic undrained strength of soils. Aio sand which is a beach sand from Yamaguchi prefecture in the south-west of Honshu in Japan was used for triaxial tests preparing with a particle size distribution of 2mm down to 74μm. The triaxial specimens of 50mm diameter and 100mm height were air pluviated to a relative density of 80%. The Samples were isotropically consolidated at mean normal effective stresses of 0.1MPa, 1MPa, 3MPa and 5MPa. Monotonic triaxial shear tests were carried out at confining pressures of 100kPa, 1Mpa, 3MPa and 5Mpa while cyclic triaxial tests were carried out at confining pressures of 100kPa, 3MPa and 5MPa. Further many sieving tests were performed at several stage of shearing by terminating the triaxial tests to determine the degree of particle breakage. The fines content was increased due to particle crushing even during undrained shear process in which the effective stress decreased. It was noted that the undrained shear behaviour was greatly dependent on the particle crushing of sands.

INTRODUCTION

In 1964 during the Niigata earthquake there was widespread damage due to liquefaction. This led to a large research effort on the liquefaction properties of silica sands. However in 1995 during the Great Hanshin Earthquake serious damage occured to port and harbour facilities such as Kobe Port Island and Rokko Island. Both of these were areas of reclaimed land filled with a crushable residual granite soil, Masado. In 1997 during the Kagoshima-ken Hokuseibu earthquake, the liquefaction of a crushable volcanic soil, Shirasu, was observed.

Research until now has concentrated on hard grained soils tested at relatively low stresses outside the crushing region. Hyodo et al. (1996) have carried out tests on the liquefaction and cyclic strength of crushable soils. However in an attempt to relate to the previous low stress liquefaction work on hard grained sands, tests have been carried out at high confining stresses on a silica sand on which much liquefaction testing has been carried out in order to examine the cyclic strength characteristics in the crushing region. Further many sieving tests were performed at several stage of shearing by terminating the triaxial tests. Variation of particle distribution curve was observed in both consolidation and shearing process.

2. MATERIAL AND TESTING METHODS

Aio sand (G_s = 2.633; e_{max} = 0.958; e_{min} = 0.582; U_c = 2.74) is a beach sand from Yamaguchi prefecture in the south-west of Honshu in Japan. The sand was prepared with a particle size distribution of 2mm down to 74μm.

[1] *Dept. of Civil Engineering, Yamaguchi University, Ube Japan, E-mail: hyodo@po.cc.yamaguchi-u.ac.jp*
[2] *Dept. of Civil Engineering, Yamaguchi University, Ube Japan, E-mail: hyodo@po.cc.yamaguchi-u.ac.jp*
[3] *Dept. of Civil Engineering, Kumamoto Institute of Technology, Kumamoto, Japan*
[4] *Dept. of Civil Engineering, University of Sheffield, UK*
[5] *Dept. of Civil Engineering, Yamaguchi University, Ube Japan*

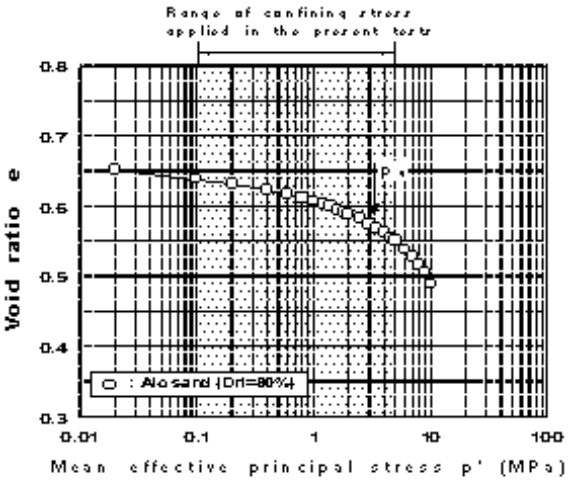

Fig.1 Isotropic compression curve for Aio sand

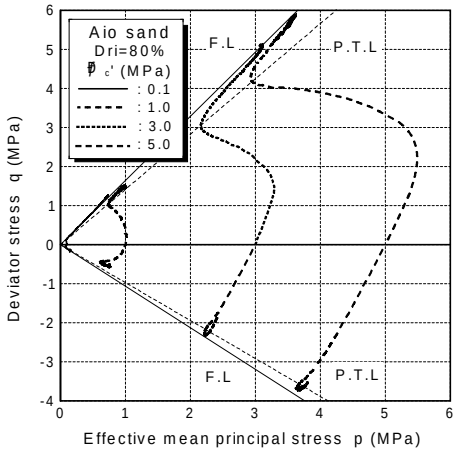

Fig.2 Effective stress path for undrained compression and extension tests with various confining stresses

Triaxial specimens of 50mm diameter and 100mm height were air pluviated to a relative density of 80% and an initial dry density γ_d of 1.589 Mg/m^3. The sample was saturated under a back pressure of 200kPa to a B value > 0.96. The isotropic consolidation curve for these samples from 20kPa to 10MPa is shown in Fig.1. The yield point, given by the point of maximum curvature, is marked on this diagram at about 3MPa. It is considered that at stresses greater than 3MPa, considerable particle crushing was initiated. Monotonic triaxial shear tests were carried out at confining pressures of 0.1MPa, 1Mpa, 3MPa and 5Mpa while cyclic triaxial tests were carried out at confining pressures of 0.1MPa, 3MPa and 5MPa with a frequency of 0.05Hz. Samples were sieved before and after testing to determine the degree of particle breakage.

3. UNDRAINED MONOTONIC SHEAR CHARACTERISTICS

Undrained compression and extension tests were carried out at each confining pressure. The effective stress paths plotted in p'-q space are shown in Fig. 2. At the low confining stress of 100kPa dilative behaviour was predominant and the stress path moved rapidly to the right from the initial stages of the test and terminated on the failure line as shown in the figure. As the initial confining pressure was increased the stress path could be characterised by three stages. Initially relatively low positive pore pressures are produced and the stress path moves to the right indicating a dilative tendency, in the second stage the compressive behaviour predominates and the stress path moves to the left until it reaches a phase transformation point. At this point it moves into the third phase of the behaviour which is characterised by a strengthening of the dilative behaviour once again and the stress path moves towards a final steady state point. At confining pressures greater than 3MPa (the yield stress on the isotropic compression curve) the stress path terminates on the steady state line with large positive pore pressures and an effective p` less than the initial confining pressure indicating net compressive behaviour. On the other hand the stress paths on the compression side for initial confining stresses of 1MPa or greater have compressive characteristics.

4. UNDRAINED CYCLIC SHEAR CHARACTERISTICS

Fig.3 shows the relationship between cyclic deviator stress and axial strain for a confining pressure of 100kPa. In this case most of the axial strain occurred in extension which is characteristic of dense sands tested at low confining pressures. This type of behaviour also indicates inherent anisotropy in the sand. Fig.4 shows a similar plot for a cyclic test at 3MPa confining pressure. Here the development of cyclic strains occurs in both compression and extension. The behaviour is very reminiscent of that for clays reported by Hyodo et al. (1994). Examination of the cyclic stress paths in each case shows cyclic mobility occurring for σ'_c= 100kPa in Fig.3 as the stress paths cycle through zero effective confining pressure. In the case of σ'_c =3MPa the mean normal effective stress do not reach zero during each cycle.

Defining cyclic failure as a strain double amplitude of 5% (ε_{DA}=5%), cyclic strength curves have been drawn for each confining pressure and are shown in Fig.5. It can be seen that the cyclic strength decreases as the

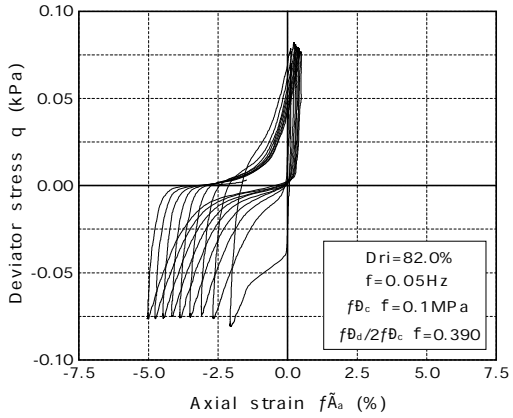

(a) Relationship between cyclic stress and axial strain

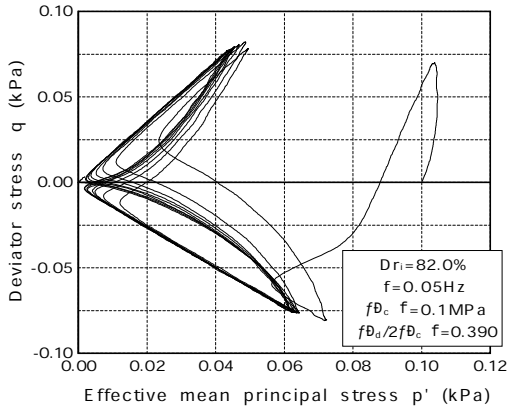

(b) Effective stress path

Fig.3 Typical cyclic stress and axial strain curve and effective stress path for a test at σ'_c=100kPa

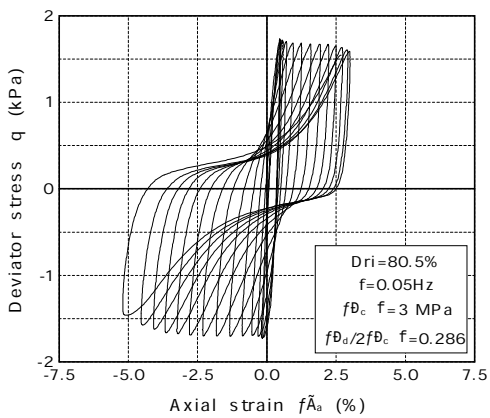

(a) Relationship between cyclic stress and axial strain

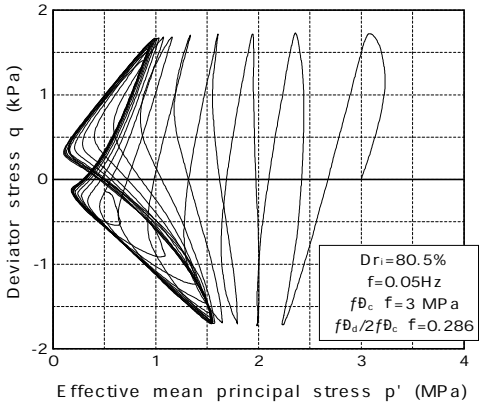

(b) Effective stress path

Fig.4 Typical cyclic stress and axial strain curve and effective stress path for a test at σ'_c=3MPa

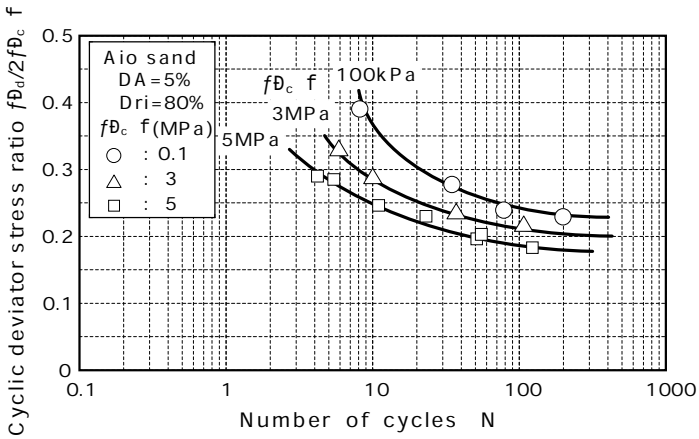

Fig.5 Cyclic strength curves for various confining stresses

confining pressure is increased from 100kPa to 5MPa. The cyclic strength curve is very steep for a confining pressure of 100kPa, which is typical of a dense sand. As the confining pressure increases to 5MPa, so the curves become flatter which is more like the behaviour of a loose sand. At low confining pressures it is accepted that the cyclic strength is independent of confining pressure (Yunoki, et al. 1982). It can be seen that at higher confining pressures where particle crushing is initiated this is no longer true.

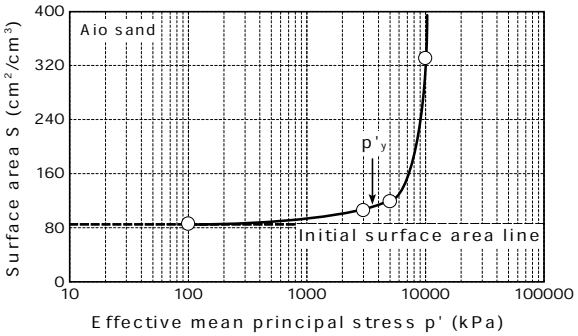

Fig.6 Variation of grain surface area with isotropic consolidation stresses

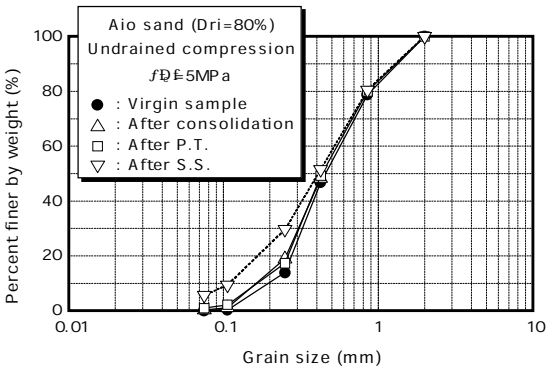

Fig.7 Grain size distribution curves for samples at the each stage of monotonic test under 5MPa confining stress

5. EFFECT OF PARTICLE CRUSHING ON UNDRAINED CYCLIC SHEAR BEHAVIOUR

In this study a method of evaluating particle crushing originally proposed by Miura and Yamanouchi (1971) was used. The method involves the quantification of the surface area of the particles. The specific surface of the particles was measured by first sieving the soil using 840μm, 420μm, 250μm, 105μm and 74μm sieve sizes. For particles larger than 74μm the following equation was used:

$$S_{w1} = \sum \frac{F}{100} \cdot \frac{4\pi (d_m/2)^2}{(4/3)\pi (d_m/2)^3 G_s \gamma_w} \qquad (1)$$

where d_m is $\sqrt{d_1 d_2}$ where d_1 and d_2 are adjacent sieve sizes (e.g. 840μm and 420μm); F is the % by weight retained on the sieve. G_s is the specific gravity of the particles and γ_w is the unit weight of water. For particles smaller than 74μm the specific surface was measured using the Blaine method for cement, using Equation (2).

$$S_{w2} = \sum \frac{F}{100} \cdot \frac{S_0 \cdot G_c \cdot t \cdot (1-e_0) \cdot \sqrt{e^3}}{G_s \cdot t_0 \cdot \sqrt{e_0^{\,3}} \cdot (1-e)} \qquad (2)$$

where: G_c is the specific gravity of the cement, S_0 is the specific surface, t_0 is a sedimentation time and e_0 is the void ratio of cement powder. The values of e and t were those for the soil as was G_s.

The overall specific surface was calculated as:

$$S_w = S_{w1} + S_{w2} \qquad (3)$$

The surface area S m^2/m^3 was obtained by the product of S_w and dry density γ_d:

$$S = S_w \cdot \gamma_d \qquad (4)$$

The variation of grain surface area with isotropic consolidation stresses is shown in Fig.6. The surface area increased rapidly after the yield stress p'_y was exceeded.

6. PARTICLE CRUSHING DURING UNDRAINED MONOTONIC SHEAR

Sieving tests were performed at several stage of shearing by terminating the monotonic triaxial shear tests. They were carried out: 1) on the virgin samples; 2) after the end of consolidation; 3) after the phase transformation point; and 4) finally after the steady state point was reached. The results for these are shown in Fig. 7. Additional sieving tests were also carried out at 10% and 15% axial strains. The particle surface area was then evaluated using the method described above. Thus Fig. 8 indicates an increase in surface area at the phase transformation state particularly at high effective confining stresses. After the phase transformation point the degree of particle crushing accelerated and continued to increase up to the steady state.

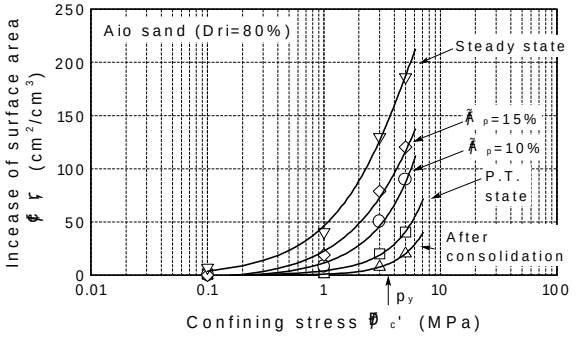

Fig.8 Increase in surface area during undrained shear at various confining stresses

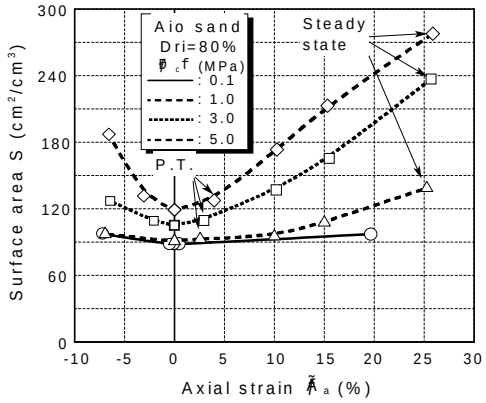

Fig.9 Variation of surface area with axial strain for both compression and extension tests

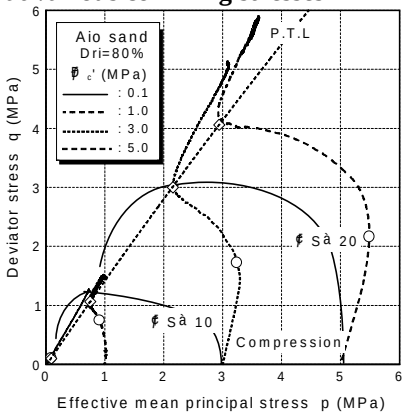

Fig.10 Contours relating to the change in surface area

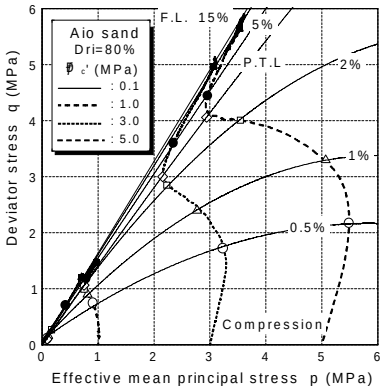

Fig.11 Contours of axial strain

Fig. 9 shows the variation of the actual surface area with axial strain for both compression and extension tests. For the lowest confining pressure the change in surface area was very small but as the confining pressure increased we can see a corresponding increase in surface area changes during testing. This increase was particularly marked after the phase transformation point and more so for σ'_c greater than or equal to 3MPa. It can also be observed however that even for the lowest occuring after consolidation at 1MPa. Thus particle crushing was more likely to occur in shear than under isotropic consolidation. Fig.2 has been redrawn as Fig. 10 but this time tentative contours relating to the change in surface area have been superimposed on this figure. There are only 3 data points for $\Delta S = 40 cm^2/cm^3$ and 2 for $\Delta S = 20 cm^2/cm^3$ and although elliptical contours have been sketched in, further extensive testing work would be needed to verify this. In the meantime it is suggested that contours of crushing may have a similar shape to the Cam Clay type of yield surface. In Fig. 11 the contours of axial strain have been drawn for the shear tests up to the PTL these are initially quite curved and widely spaced but after the PTL they become straighter and as might be expected more closely spaced. Up to 0.5% strain in Fig. 10 the stress paths are dilative and only small amounts of crushing occur as the stress path approximately follows the contours for ΔS. Up to this point there is no breaking of asperites and the magnitude of the strain can be accounted for by particle rearrangements with movements of the same order as small asperites. It should also be noted that the degree of dilatancy increased with effective consolidation stress and hence density. From 0.5% to the PTL at 3% to 4% strain the stress paths became compressive. Over this region it is postulated that there was some breaking of small asperites. From the PTL line to the steady state the direction of the stress paths became dilative and axial strains greater than 10% were measured. It is thought that this third phase was accompanied by major particle breakage and rearrangement particularly at higher confining stresses.

7. EFFECT OF UNDRAINED CYCLIC SHEAR ON PARTICLE CRUSHING

The degree of particle crushing after cyclic loading was measured using the above technique. The samples were cycled until a 10% double amplitude strain was reached after which the surface area was re-determined. The results are shown in Fig. 12. The data for isotropically consolidated samples where $\sigma_d/\sigma_{2c} = 0$ is also included. For $\sigma'_c = 100kPa$ there is no significant change during a cyclic test. On the other hand for the high stresses in the

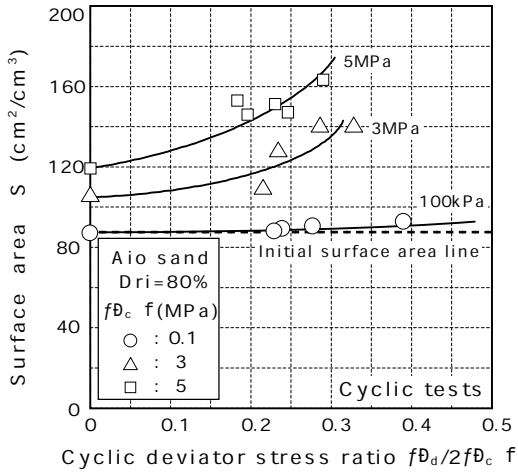

Fig.12 Degree of particle crushing after cyclic loading

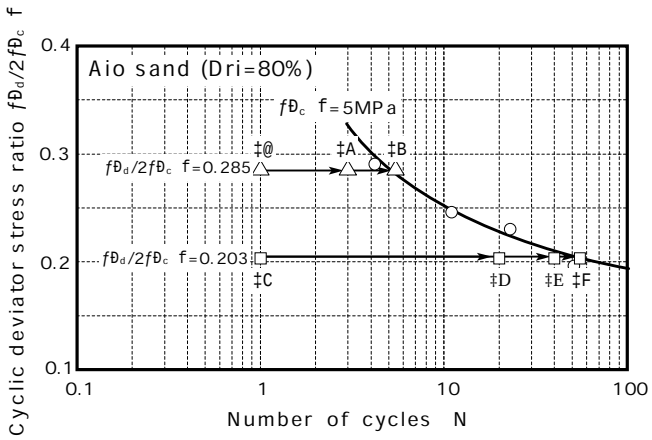

Fig.13 Relationship between cyclic deviator stress ratio and the number of cycles to reach ε_{DA} =5% and the number of cycles at which the separate tests were terminated to measure particle crushing

crushing region the surface area increases with increasing applied cyclic stress ratio and confining pressure σ'_c . It is interesting to note that even though during a cyclic loading test the effective stress was decreasing, unlike isotropic consolidation where the effective stress was increasing considerable particle crushing still occurred.

In order to observe the development of particle crushing during a cyclic loading test, a number of tests were carried out which were terminated either after a given number of cycles or when certain critical stages were reached such as the phase transformation line (Hyodo et al., 1998) or a 5% double amplitude strain (Fig. 13). This figure also includes the lines showing the relationship between cyclic deviator stress ratio and the number of cycles to reach ε_{DA} =5% . Fig. 13 shows the number of cycles at which the separate tests were terminated. These tests were carried out at an effective confining pressure of 5MPa which is well above the soils yield stress.

Fig. 14 shows the development of the surface area S for the different tests shown in Fig. 13. In this figure the phase transformation and ε_{DA} =5% states are shown by dotted lines and associated stress paths for each of the tests are shown together with this figure. The degree of particle crushing as might be expected increased with increasing cyclic stress ratio. It can also be seen that after the phase transformation state was reached the particle surface area increased rapidly. This was because after the phase transformation point large strains occurred with associated translation and rotation of particles causing the higher degree of crushing.

8. CONCLUSIONS

Undrained monotonic and cyclic triaxial tests have been carried out at low and high confining stresses up to 5MPa on a silica sand in order to examine the shear behaviour in the crushing region.

1) The isotropic consolidation curve indicated that yielding occurred at about 3MPa and considerable particle crushing occurred at stresses in excess of this value. Crushing was measured by sieving the samples before and after testing and determining the increase in particle surface area.

2) In monotonic shear tests, as the initial confining pressure was increased the stress path could be characterised by three stages. Initially relatively low positive pore pressures are produced and the stress path moves to the right indicating a dilative tendency, in the second stage the compressive behaviour predominates and the stress path moves to the left until it reaches a phase transformation point. At this point it moves into the third phase of the behaviour which is characterised by a strengthening of the dilative behaviour once again and the stress path moves towards a final steady state point.

3) Cyclic stress paths for the dense sand at high confining pressures were similar to those observed for clays. In addition at higher confining pressures the cyclic strength curves were similar to those for loose sands at low confining pressures. In contrast to loose sands however they were dependent on the confining pressure due to particle crushing occurring during cyclic shearing.

4) Under isotropic compression the particle surface area increased rapidly after the yield stress was exceeded. In the cyclic tests there was no significant increase in surface area for the low confining pressure of 100kPa. At high stresses however the surface area increased with increasing cyclic stress ratio.

5) Surface area measurements were also carried out on several samples where the tests were terminated at the

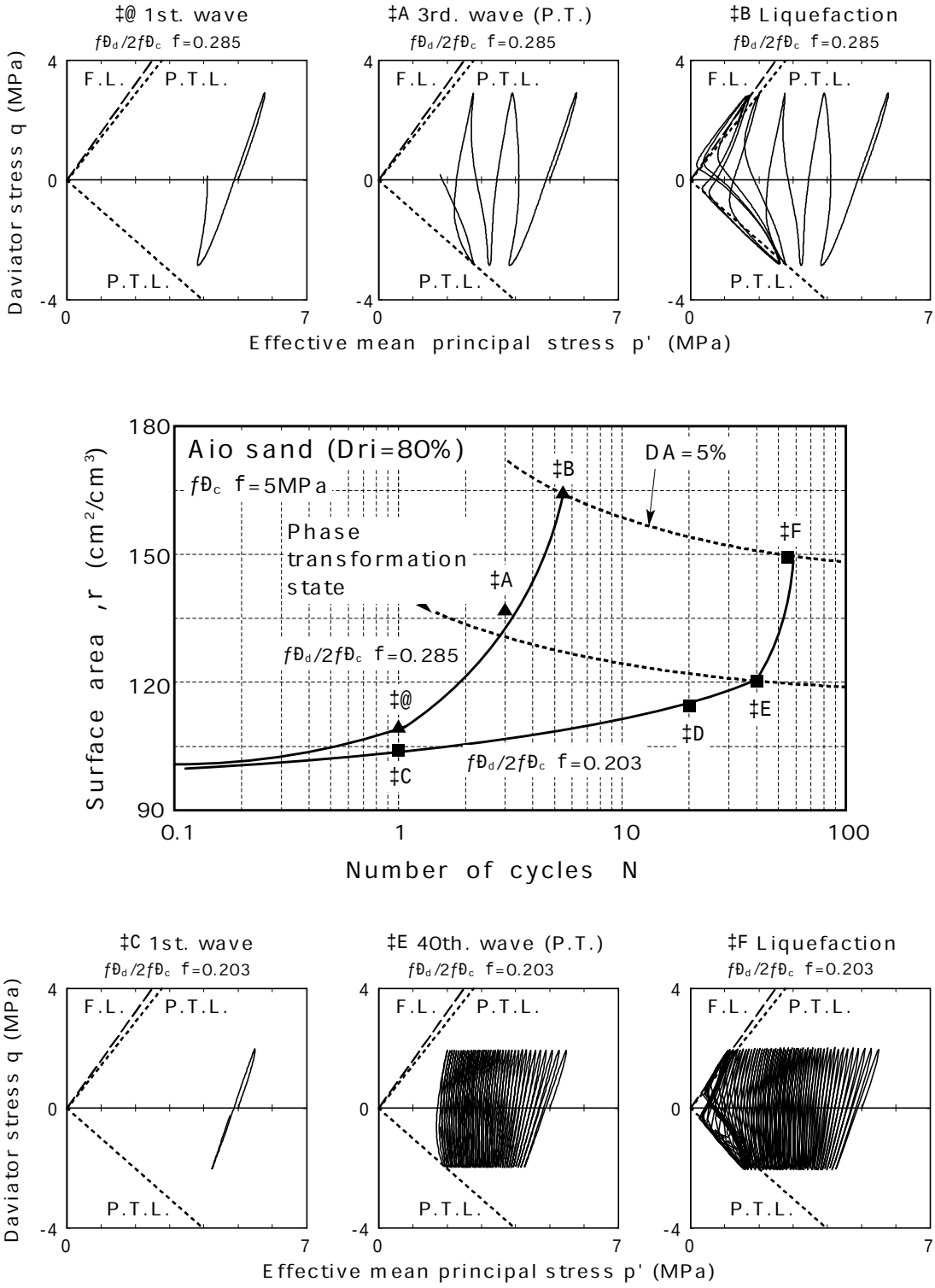

Fig.14 Relationship between grain surface area and number of cycles during undrained cyclic shear tests

phase transformation line or ε_{DA} =5%. The surface area and hence crushing was seen to increase rapidly for tests taken past the phase transformation state. At this point the development of high strains was initiated and it is thought that particle rotation and translation contributed to the crushing process.

REFERENCES

Hyodo, M., Yamamoto, Y. and Sugiyama, M. (1994), "Undrained cyclic shear behaviour of normally consolidated clay subjected to initial static shear stress." *Soils and Foundations*. 34(4): 1-11.

Hyodo, M., Aramaki, N., Itoh, M. and Hyde, A.F.L. (1996), "Cyclic shear strength and deformation of crushable carbonate sand." *Soil Dynamic and Earthquake Engineering*. 15(5): 331-336.

Hyodo, M., Hyde, A.F.L. and Aramaki, N. (1998), "Liquefaction of crushable soils." Geotechnique. 48(3): 1-17.

Miura, N. & Yamanouchi, T. (1971), "Drained shear characterisics of Toyoura sand under high confining stress." *Proc. of Japanese Society of Civil Engineers*. 260: 69-79.

Yunoki, Y., Ishihara, K.. and Seki, M. (1982), "The effect of the initial effective confining pressure on cyclic triaxial shear behaviour of dense sand." *Proc. 17th Japanese Annual Meeting on Geotechnical Engineering*:1649-1653